We are IntechOpen, the world's leading publisher of Open Access books Built by scientists, for scientists

6,900
Open access books available

185,000
International authors and editors

200M
Downloads

Our authors are among the

154
Countries delivered to

TOP 1%
most cited scientists

12.2%
Contributors from top 500 universities



WEB OF SCIENCE™

Selection of our books indexed in the Book Citation Index in Web of Science™ Core Collection (BKCI)

Interested in publishing with us?
Contact book.department@intechopen.com

Numbers displayed above are based on latest data collected.
For more information visit www.intechopen.com



Chapter 9

Piezoelectric Materials in RF Applications

Philippe Benech and Jean-Marc Duchamp

Additional information is available at the end of the chapter

http://dx.doi.org/10.5772/63125

Abstract

The development of several types of mobile objects requires new devices, such as high-performance filters, microelectromechanical systems and other components. Piezoelectric materials are crucial to reach the expected performance of mobile objects because they exhibit high quality factors and sharp resonance and some of them are compatible with collective manufacturing technologies. We reviewed the main piezoelectric materials that can be used for radio frequency (RF) applications and herein report data on some devices. The modelling of piezoelectric plates and structures in the context of electronic circuits is presented. Among RF devices, filters are the most critical as the piezoelectric material must operate at RF frequencies. The main filter structures and characterisation methods, in accordance with such operating conditions as high frequencies and high power, are also discussed.

Keywords: radio frequency, filters, MEMS, modelling, characterisation

1. Introduction

1.1. Radio frequency (RF) applications and challenges

The market of connected mobile objects, such as smartphones, tablets, notebooks, printers and television sets, among others, is always growing. In the future, an increasing number of apparatus will be connected — not only mobile objects but also stationary objects both at home and in the office. Most of these objects use multiband and multistandard in order to select the best transmission standard in accordance with their location. Therefore, they are all made subject to environments where multiple communication standards, using different frequency bands, are available. One of the main problems in ensuring high-quality communication and guaranteeing high data flow is reducing or vanishing interferences between bands during the communi-

INTECH
open science | open minds

© 2016 The Author(s). Licensee InTech. This chapter is distributed under the terms of the Creative Commons Attribution License (http://creativecommons.org/licenses/by/3.0), which permits unrestricted use, distribution, and reproduction in any medium, provided the original work is properly cited. CC BY

cation. In parallel, some of the objects listed above include functionalities in order to propose other services, such as positioning and movement detection, sometimes in complement with information coming from radio links. Many functions use piezoelectric materials. From a radio communication point of view, important devices require piezoelectric materials to reach their desired characteristics. A typical radio transceiver is presented in **Figure 1**. Such materials allow for the identification of various functions needed for the operation of devices; those that require the use of piezoelectric materials include filters, duplexers, oscillators and in complement microelectromechanical systems (MEMS), switches and so on. Among these functions, one of the most critical is filtering. The requirements to ensure no overlap from upstream and downstream bands for example are very difficult that without piezoelectric materials it is impossible to run an efficient filter and overall an efficient transmission system. This is due to the limited number of frequency bands in the same area and consequently to the limited number of usable channels. Another important challenge is the ability to use multiple communication standards with one device. The latest generation of mobile phone can use more than 15 communication standards, distributed over about 10 frequency bands. Due to the limited available space inside mobile objects' packages, it is impossible to integrate a transceiver for each frequency band. Consequently, some components will be able to be tuned dynamically to adapt to several frequency bands. Examples of frequency bands that can be used in mobile radio communication systems are given in **Table 1**. In this context, piezoelectric materials are unavoidable and are the best candidates to ensure a high-quality transmission system.

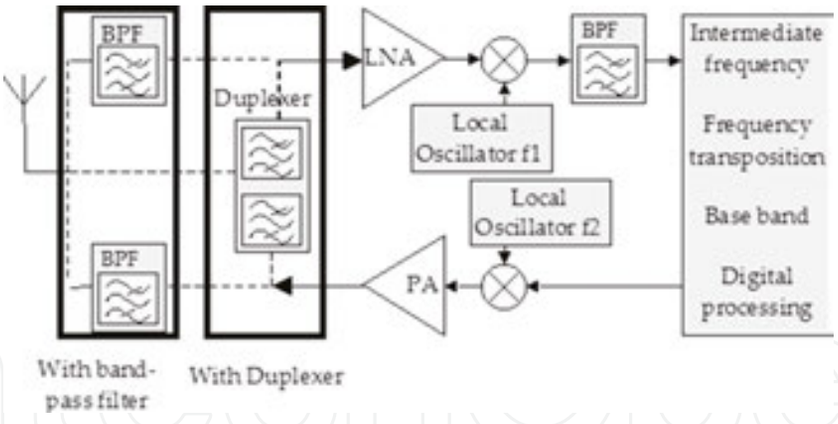


Figure 1. Schematic of a full duplex transceiver system.

Standards	Frequency range (MHz)
LTE	791–862
GSM	880–960
DVB-H	1452–1492
GPS	1575.42 and 1227.60
GSM DCS	1710–1880

Standards	Frequency range (MHz)
UMTS	1920–2170
Bluetooth	2400-2483.5
WLAN	2401–2483
LTE	2500–2690
WLAN	3655–3695
WLAN	5170–5835

Table 1. Examples of radio communication bands for mobile systems.

The evolution of RF MEMS is needed for the expanding data rate (Copper Law) and broadband wireless radio communications (**Figure 2**). This technology should be developed in parallel with the miniaturisation of the CMOS following "More Moore", together with the diversification technologies of "More than Moore" as presented by Oita [1]. This chapter will try to demonstrate the extremely high motivation for RF MEMS.

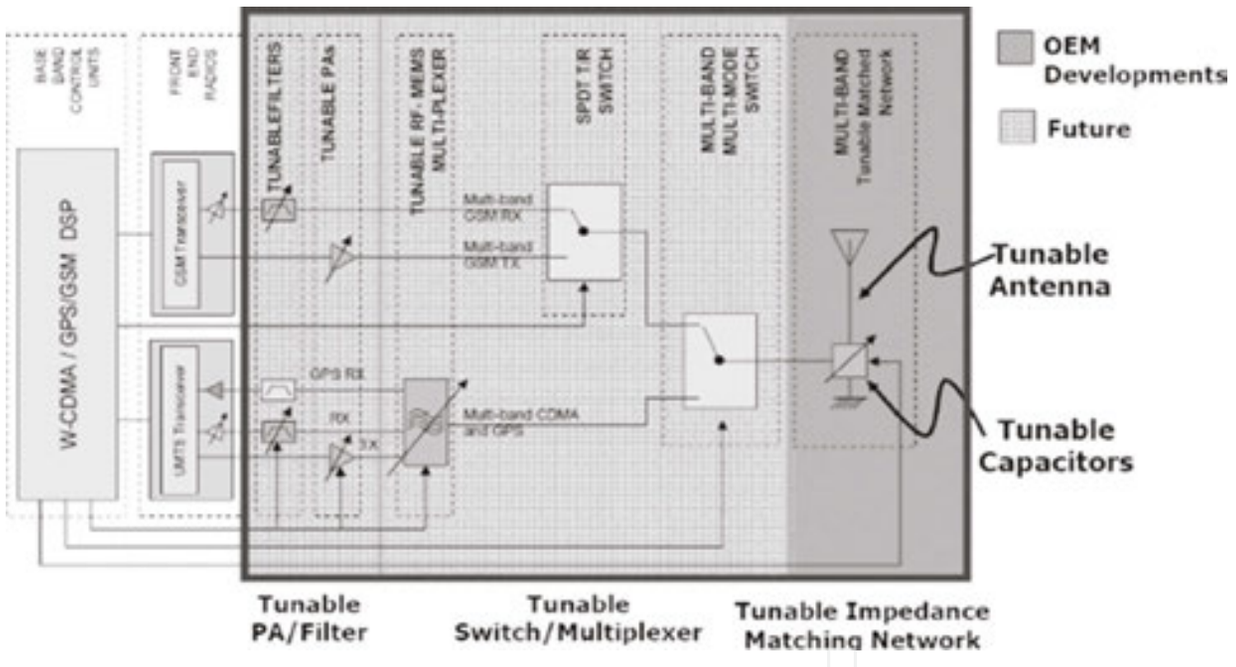


Figure 2. Programmable front end proposed by Oita [1].

A study on scientific papers published with the keywords "piezoelectric" and "RF" or "microwave" applied in RF applications over the last 50 years is first presented herein. We performed our search using the most common databases of scientific publications.

More than 300,000 papers have been published since 1965 (called "RF_papers") with the keywords "radio frequency" and "microwave". Over the years, around 850 papers (called "Piezo_papers") have focused on piezoelectric innovations in the field of RF.

The evolution of the ratio of "Piezo_papers" in "RF_papers" in percentage versus years is shown in **Figure 3**.

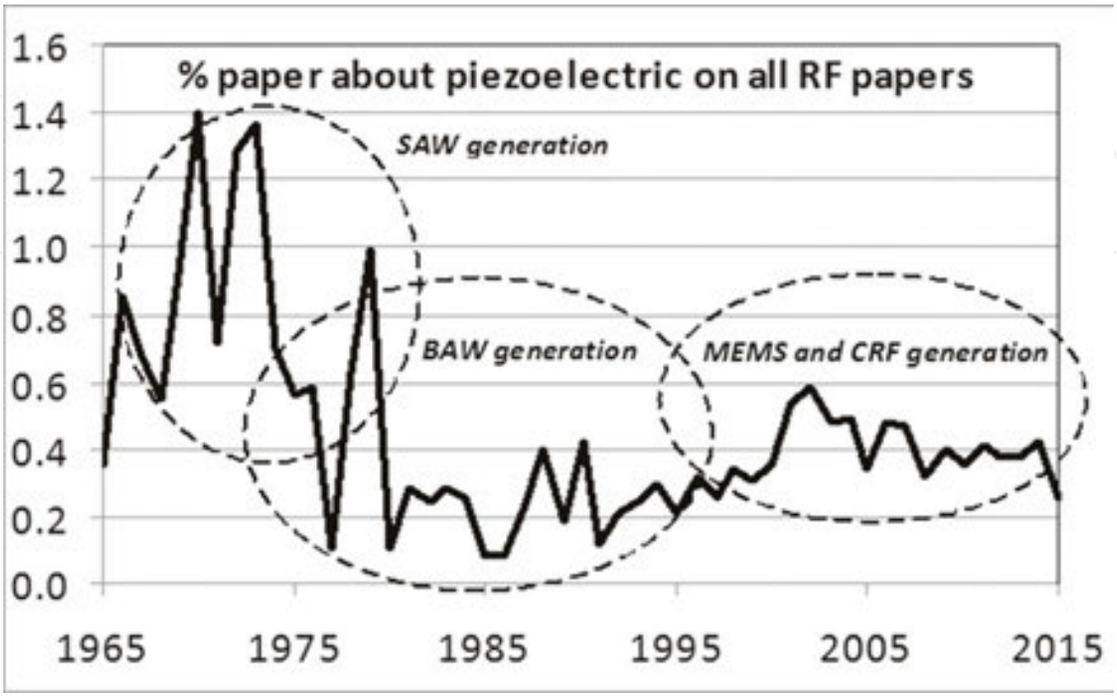


Figure 3. Evolution of the ratio of "Piezo_papers" in "RF_papers" in percentage versus years.

We noticed three periods of publications associated with three generations of RF filters or resonators.

The first peak was detected around 1970, with 1.4% of "RF_papers" dedicated to "piezoelectric" innovation. This peak describes the first generation of piezoelectric resonators or acoustic wave resonators, called surface acoustic wave (SAW) filters. The principle behind it was described for the first time in 1964 by Tehon and Wanuga [2]. A few years later, at the end of 1976, a second generation with bulk acoustic wave (BAW) filters appeared, and it was first described by Yao and Young [3]. Even if the principle was presented early, SAW filters have been serving the mobile phone market for 20 years, while the first commercial BAW filters, more precisely film bulk acoustic resonators (FBARs), were introduced in 2001 [4]. At the end of the 1990s, the maturity of and improvements in microelectronic technologies allowed for the integration of complex multilayer structures and MEMS, representing the third generation.

These different technologies of piezoelectric resonators will be described more precisely in this chapter.

The principal use of piezoelectric materials in RF applications is the design of efficient resonators with a very high quality factor for a small surface. As shown in **Figure 4**, more than 50% of published papers on piezoelectric materials in RF applications since 1980 are dedicated to improvements in resonators or filters.

http://dx.doi.org/10.5772/63125

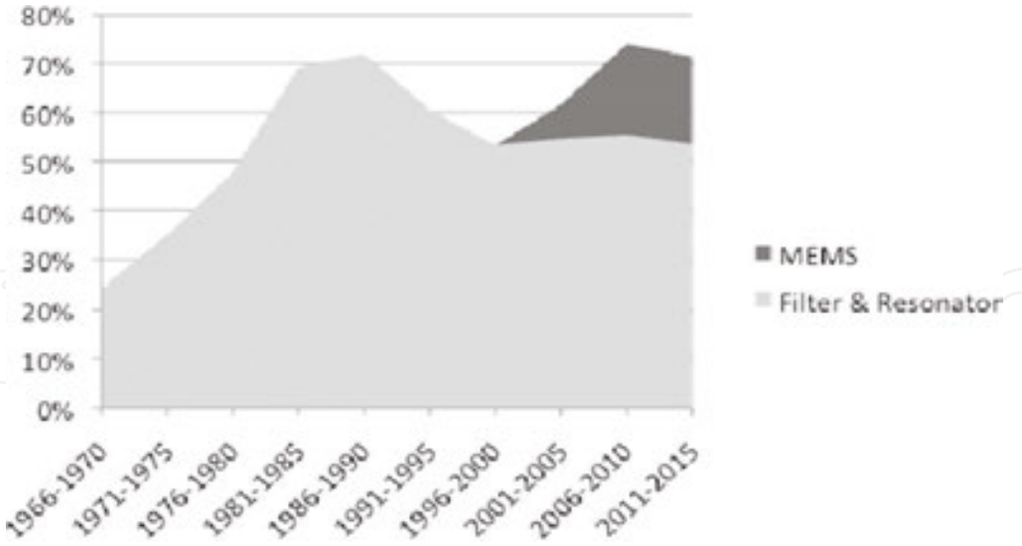


Figure 4. Topics of published papers on piezoelectric materials for RF applications.

In the last decade, new functions were proposed and described in 18% of the "Piezo_papers", based on the MEMS structures (these papers are called "MEMS_papers").

These new RF functions available, owing to MEMS structures, are switches, sensors and phase shifters. The bibliography gives the percentages of these new RF functions in published papers over the last 10 years. This repartition is shown in **Figure 5**. Published papers on piezoelectric MEMS switches for RF applications represent half (47%) of the "MEMS_papers" when innovation on piezoelectric MEMS varactors and phase shifters are respectively equal to 31% and 10% of the "MEMS_papers" about 90 papers published on the last decade.

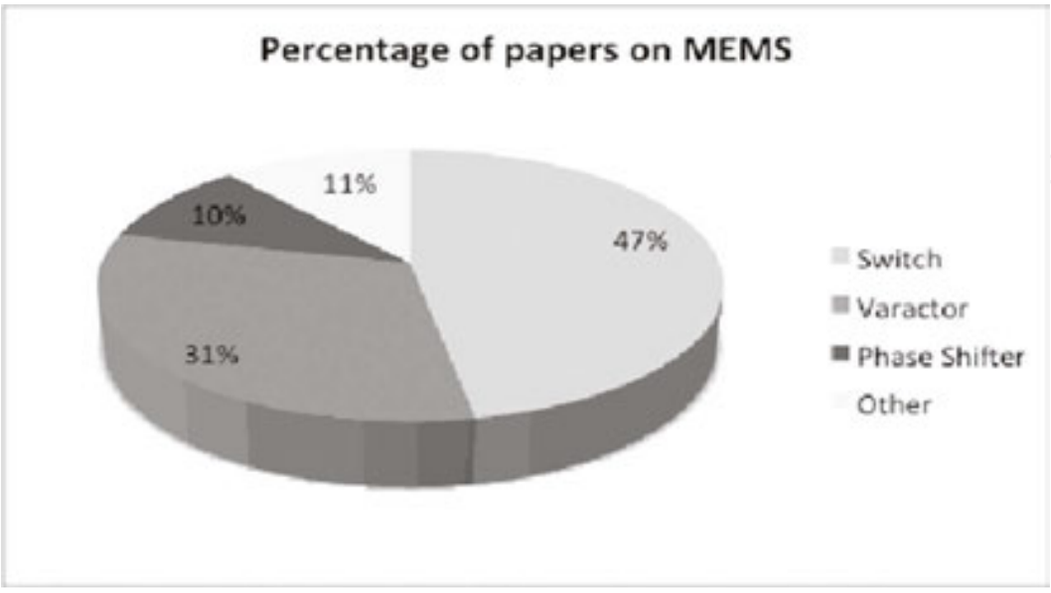


Figure 5. Topics of published papers on MEMS and piezoelectric materials for RF applications in the last decade.

This chapter is organised in three parts. First, a brief summary of the properties of various piezoelectric materials is presented. The second part describes the principal use of piezoelectric materials for RF applications: filters and resonators. The third part is dedicated to the new and emerging RF functions available owing to MEMS technology on piezoelectric materials: switches, phase shifters and varactors.

1.2. Piezoelectric materials and key parameters

For RF applications, two types of piezoelectric materials can be identified: those that will not be crossed by the RF signal and those that are in direct contact with the RF signal. For applications where the piezoelectric plate must operate in the gigahertz range, few materials can be used. The principal parameter for selecting a piezoelectric material is the means of production and compatibility with technological processes similar to those used in microelectronics. Another parameter is the maximum frequency of operation with a good quality factor.

A material is defined by several physical parameters, such as piezoelectric constants, stiffness, complex dielectric constants and other constants. End users of piezoelectric materials are more interested in other parameters, such as the electromechanical factor, the deposition process, which influences piezoelectric behaviour, the ability to hold up high RF power, and consequently nonlinear behaviour, the maximum frequency of operation. This list is not exhaustive and can be extended in accordance with use. Limited data about the characteristics of piezoelectric materials submitted to high RF power are available in the literature. Moreover, many results suggest that thin film exhibits better characteristics than bulk materials and that the coupling factor, the piezoelectric constant and other parameters are dependent on the fabrication process. It is difficult to obtain the absolute values of parameters, such as piezoelectric constants, mechanical stiffness and so on. Despite this, it is interesting to determine their important characteristics based on the available literature data to compare piezoelectric materials.

Table 2 shows the square values of the coupling factor k_t^2 and the mechanical quality factor values in the gigahertz range. These two parameters are often used as figures of merit. These materials are lead free except for PZT. This last material will probably be removed from the composition of devices according to regulations in several countries. Another important characteristic will be the tunability of the resonance of the piezoelectric plate. This will be a challenge for the future due to the great number of standards and the limited space in a mobile object. The ideal filter can be electrically tuned and adapted to several frequency bands. Some materials, such as barium strontium titanate (BST), have been used to realise a tunable filter. Although at this time, tunability is limited to a small percentage of the central frequency and can only compensate the variability of process fabrication. At this time, AlN offers the best trade-off, but it cannot be electrically tuned. However, it is possible to improve the properties of AlN by substituting a part of Al with Sc; this mainly leads to an increase in piezoelectric coefficients.

Material	k_t^2 (%)	Q (frequency of measurement)
AlN [4]	7	2000 (2 GHz)
$Al_{0.88}Sc_{0.12}N$ [5]	7,5	650 (2.5 GHz)
$(Mg_{0.5}, Zr_{0.5})_{0.13}A_{10.87}N$ [6]	8.5	808 (2 GHz)
$(Mg_{0.5}, Hf_{0.5})_{0.13}A_{10.87}N$ [6]	10.0	781 (2 GHz)
BST [7]	7	230 (2 GHz)
GaN [8]	1.7	210 (2.1 GHz)
$(K_{0.5}Na_{0.5})NbO_3$ [9]	61	240 (~MHz)
$LiNbO_3$ [10]	20	1000 (2 GHz)
$LiTaO_3$ [11]	20	1000 (2 GHz)
PZT [12, 13]	9.61	237 (2 GHz)
ZnO [13]	9	1770 (2 GHz)

Table 2. Characteristics of the most used piezoelectric materials.

2. Piezoelectric filters

The first filter type was the SAW filter. Probably one of its most important characteristics is the accuracy of the resonant frequency of the structure. Microelectronic technology offers a good resolution to realise the structure in the plane of the substrate, but thickness control is more difficult. As thickness is crucial to bulk resonance mode, without a minimum of accuracy to control the thickness, the resonant frequency will sweep as it is directly linked to the thickness. This is probably one of the most important reasons to use a SAW filter as this type of filter does not require high accuracy for piezoelectric plate thickness. SAW filters require only the control of the dimensions of interdigital transducers (IDTs), particularly the finger's width and the shape of the finger that must exhibit very low deviation compared with the mean value. Nevertheless, SAW filters occupy a more important area than other filter types.

2.1. Surface acoustic wave (SAW) filter

The technological steps to realise a SAW transducer are restricted to the depositing of a metal layer that is then etched to obtain the final electrodes on the surface of the piezoelectric plate. This technology was first used for delay lines and for bandpass filters.

2.1.1. Principle

The basis of this type of filter is the generation of a well-known SAW. Among SAWs, the Rayleigh wave that exhibits the same behaviour is preferable because for propagation direction and the wave velocity is independent of the frequency. Nevertheless, it implies that the propagation path has a thickness two times higher than the wavelength and this condition

cannot be satisfied in any case. Thus, Lamb waves [14] are more often generated. This type of filter is based on a piezoelectric plate deposited on substrate (silicon, alumina and so on). A pair of IDT is etched at the top. One will be excited by the input signal, and the other one will receive the acoustic wave generated by the first one. **Figure 6** shows the basic requirements for a bandpass filter. The distance between two adjacent fingers must be half the wavelength (**Figure 7**). The frequency of operation and consequently the filter characteristics are dependent on the dimensions of IDTs. The higher the number of fingers of the transducer, the greater the selectivity of the filter and the more the bandwidth is reduced.

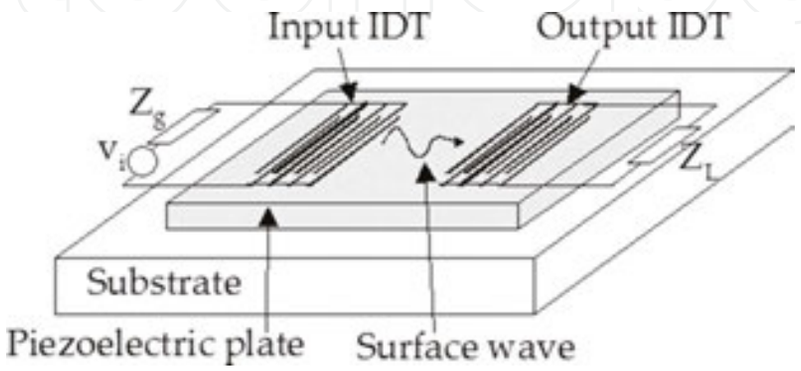


Figure 6. Basic SAW filter.

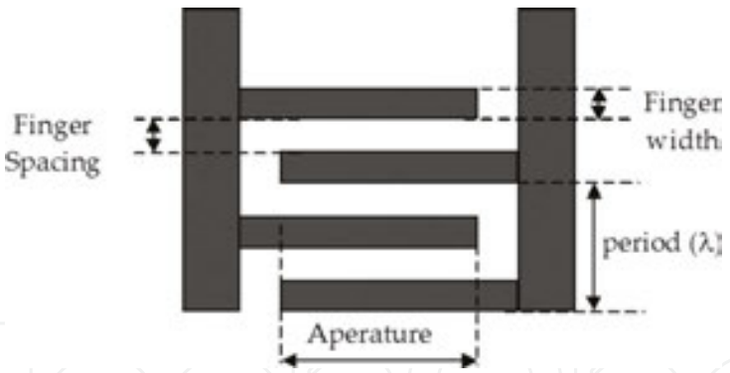


Figure 7. IDT specifications.

2.1.2. Topologies

On the basis of an IDT, several research studies were conducted to improve the characteristics of filters. It is possible to use different configurations by changing the way IDTs are coupled, by adding attenuators or reflectors at both ends of the surface of the piezoelectric plate. It is also possible to select specific materials to compensate the temperature variation of the piezoelectric layer and to minimise the characteristics of the shift [15].

The longitudinally coupled IDT shown in **Figure 8(a)** is probably the most used, but it requires reflectors to improve coupling or in other cases attenuators to reduce spurious wave propa-

http://dx.doi.org/10.5772/63125

gation on the substrate surface [16]. It is also possible to use transverse coupling [17], but this configuration is more difficult to operate (**Figure 8(b)**). Finally, the association of several transmission SAW structures can be done as shown in **Figure 8(c)** to improve filter characteristics. However, the main drawback is the occupied surface that is increased by the number of SAW devices. Although SAW devices exhibit advantages, in terms of fabrication, their surface is a handicap. Nevertheless, this type of filter is always used in commercial products.

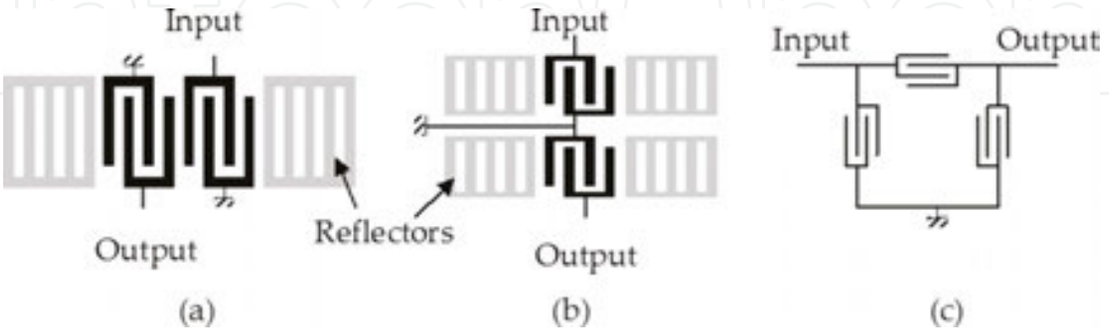


Figure 8. Main structures based on SAW: (a) longitudinal coupling; (b) transverse coupling; (c) ladder structure.

2.2. Bulk acoustic wave (BAW) filters

2.2.1. Bulk acoustic wave resonators

A piezoelectric plate surrounded by metal electrodes is excited in almost all structures in thickness resonance mode to realise a BAW structure. Different arrangements can be done using this basic plate. The principal problem is to keep the properties of the piezoelectric layer as the quality factor. The main constraint is the control of the thickness of the piezoelectric layer as it defines the resonance frequency of the final structure. The piezoelectric layer must be placed on a substrate. The substrate has a significant role in ensuring a high quality factor. It must have a low acoustic impedance compared with the piezoelectric layer. Two main possibilities are used to reach this goal: The first structure, FBAR, is realised on a membrane below which an air cavity is created by micro-machining to ensure a good acoustic reflection. The main drawbacks of FBAR are the complex process to realise the air cavity and the fragility of the devices. The second structure is a solidly mounted resonator (SMR) where the piezoelectric layer and its electrodes are placed on a Bragg acoustic reflector. For both structures, a final layer is deposited at the top and its thickness is adjusted to reach the right resonant frequency. These filters have been highly improved compared with SAW filters, but they remain sensitive to temperature variations and to high power [18].

2.2.2. Film bulk acoustic resonator (FBAR)

A schematic presentation of an FBAR cross-section is given in **Figure 9**. The device is composed of a piezoelectric thin film sandwiched between two metallic electrodes, and the bottom one is deposited on an acoustic isolation. The top electrodes can be apodised to minimise spurious

modes. A good acoustic isolation is realised by an air cavity underneath the membrane released by bulk micromachining [19, 20].

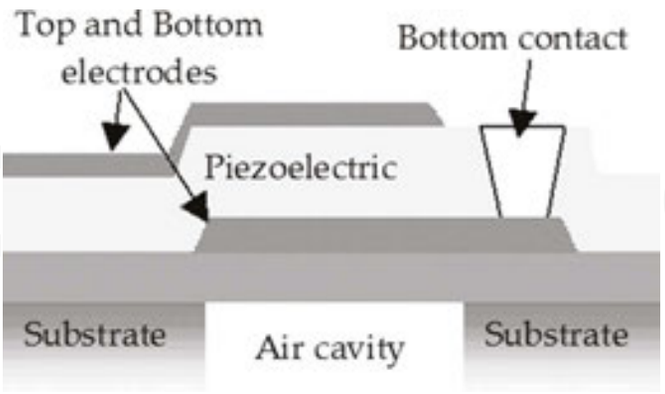


Figure 9. FBAR structure.

2.2.3. Solidly mounted resonator (SMR)

For a SMR, the air cavity is replaced by a Bragg mirror as shown in **Figure 10**.

The transpose of a method widely used in optics, which is the Bragg mirror, consists of producing alternating stacks of materials of quarter-wave layers havingwith low and high acoustic impedances under the active part of the resonator. This principle allows to obtain reflected waves in-phase with the incident waves generated by the piezoelectric plate to ensure a high quality factor of the structure. The advantages of this structure relative to FBAR are the mechanical strength and the manufacturing process, which is simpler. This structure, however, requires the deposition of additional layers for the Bragg mirror.

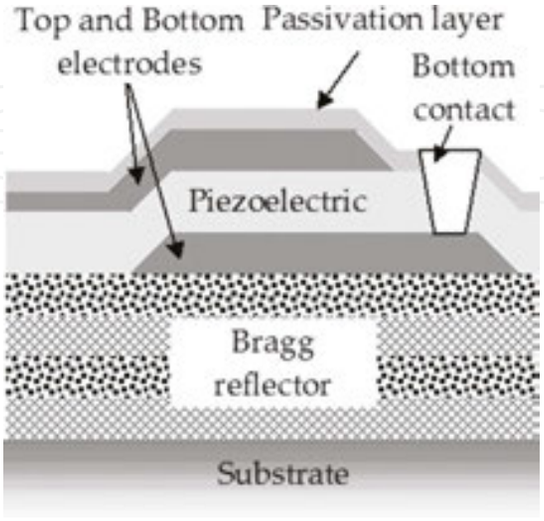


Figure 10. SMR structure.

http://dx.doi.org/10.5772/63125

2.2.4. Filter topologies

BAW resonators (FBAR or SMR) are arranged side by side to realise a filter, which simplifies the manufacturing process insofar as a single piezoelectric layer is necessary. However, this category of BAW filters does not allow mode conversion, from asymmetric mode to differential mode, or impedance transformation. Two main architectures of filters exist, ladder filters "Π" or "T" as shown in **Figure 11(a)** and lattice as shown in **Figure 11(b)**. It is necessary to have two types of resonators having different resonant frequencies to build these filters (**Figure 12**). The frequency shift can be obtained by adding an additional layer on top of the standard resonator to lower the frequency or by etching the top layer of the stack to increase the frequency. This frequency shift is of great importance in the manufacture of such filters since it determines the width of bandwidth and the level of insertion loss. In **Figure 12**, the transmission coefficient of a ladder structure is presented with the impedances of both resonators. The resonance of the series resonator gives the lower limit of the passband, while the resonance of the shunt resonator gives the upper limit of the passband.

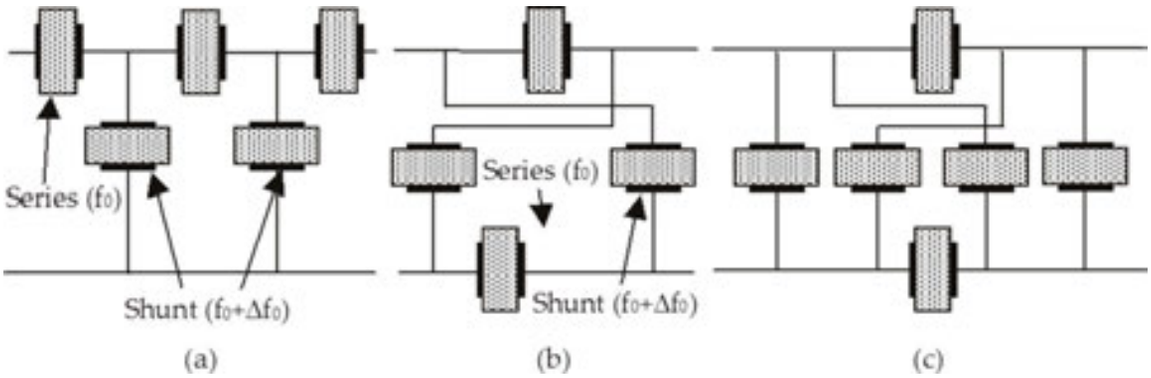


Figure 11. Topologies: (a) ladder; (b) lattice; (c) mixed.

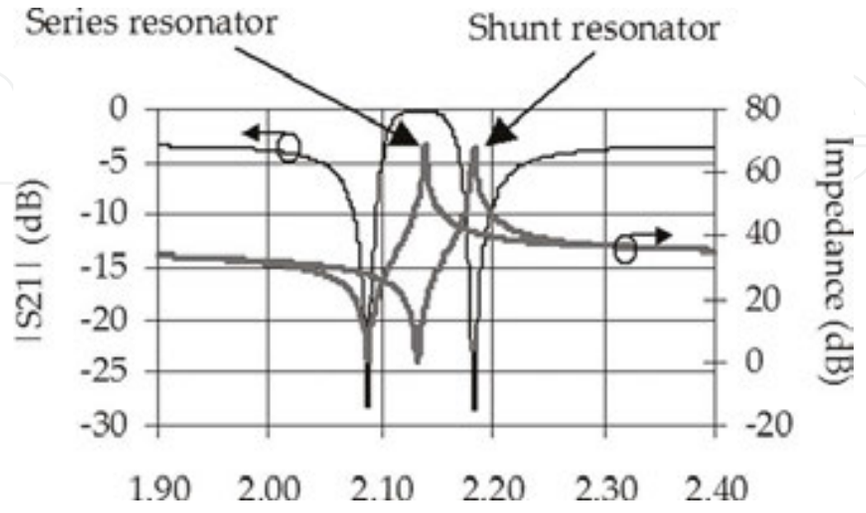


Figure 12. Transmission coefficients of a ladder structure with two resonators.

The ladder network has a common ground between the inlet and the outlet. The disadvantage of lattice filters is their poor transition band (**Figure 13**) in comparison with ladder filters and with the same number of resonators. It is possible to combine both architectures in a mixed ladder-lattice architecture to combine the advantages of both topologies [21] (**Figure 11(c)**), allowing for the integration of the performance of selectivity and out-of-band rejection of the two topologies.

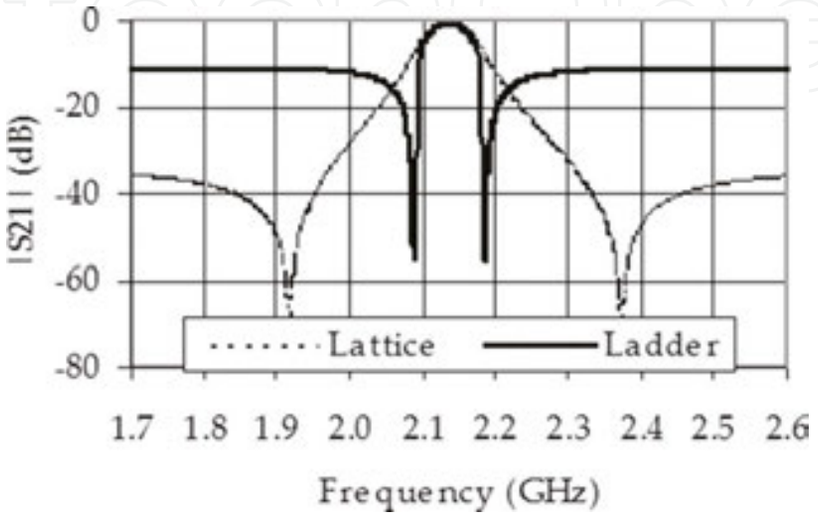


Figure 13. Transmission coefficients of a ladder and ladder filters.

2.3. Coupled resonator filter (CRF)

The CRF was proposed by Lakin [22] in 2002. This filter is based on three resonators acoustically coupled as shown in **Figure 14**. The input resonator is excited in thickness mode. The acoustic wave will propagate toward the lower resonator through the three coupling layers, guaranteeing optimal transmission between upper and lower piezoelectric layers. The lower piezoelectric layer generates an electric field by the inverse piezoelectric effect, which will be guided to the second stack through the continuous electrode of the lower piezoelectric layer. The lower resonator of the second stack, excited by an electric field, emits an elastic wave that travels upward with the coupling layers. This acoustic wave reaches the upper right resonator to finally generate an electric field and the filter output voltage. This structure exhibits a bandwidth comparable with or higher than SAW. As shown in **Figure 15**, the transmission coefficient reaches values lower than −80 dB before and after the passband, whereas for BAW filters, **Figure 13** shows that the transmission coefficients, after having reached values higher than -80 dB at the ends of the passband of the filter, increase to values between −40 and −10 dB. The out-of-band rejection of CRFs is better than that of BAW filters. The fabrication process of this filter is fully compatible with the microelectronic process. It is possible to realise these filters as stand-alone devices or as integrated components. With this type of filters, it is possible to realise impedance matching by changing the dimensions of the input resonator or output resonator, except the thickness. A balanced-unbalanced transformation [23], which is not

http://dx.doi.org/10.5772/63125

possible with ladder or lattice structures, can also be designed. Finally, it occupies the smallest surface as compared with other acoustic filters.

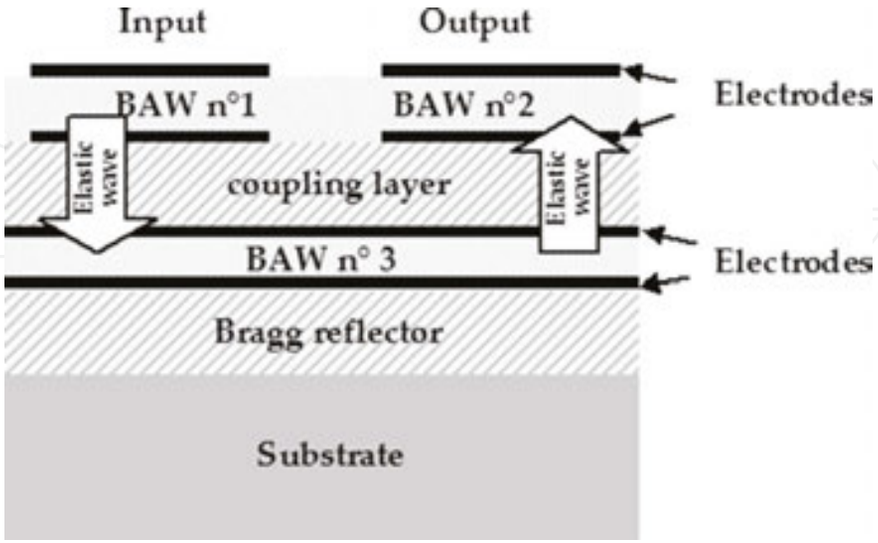


Figure 14. CRF structure.

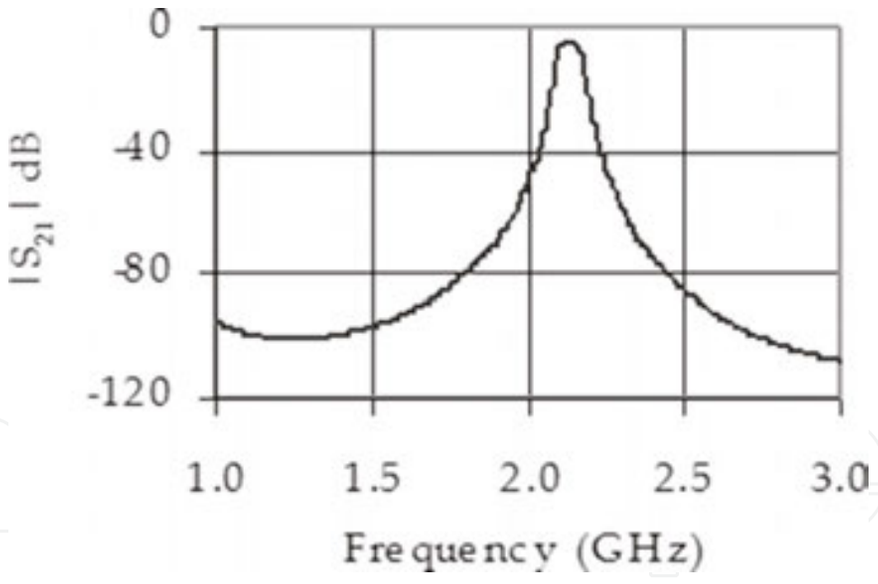


Figure 15. Simulated transmission coefficients of CRFs.

2.4. Modelling of piezoelectric filter

Modelling of piezoelectric devices can be achieved in different ways. It depends mainly on the wanted result. The first option is to use a finite element software that is based on 3D modelling. Over the past few years, some commercial software programs were proposed. In general, they are more oriented toward mechanical behaviour analysis, giving information about resonance

modes, strain, displacement and other mechanical information. They are more or less difficult to use according to the machine interface. Most of them can give excellent results on the condition that the user will control, for example, boundary conditions and other features. Another option is to use 1D models, such as the Butterworth-Van Dyke (BVD) circuit, KLM [24], Mason's model and the transmission line model [25]. Its main advantage is that these models can give information about the electrical behaviour of piezoelectric materials. This is important when the piezoelectric plate is included in an electronic circuit, such as for telecommunications transceivers. The main drawback of this option is that 1D models can only be powerful in one dimension and consequently for one vibration mode of the piezoelectric plate. Each model has advantages and drawbacks. The basic BVD model (**Figure 16**) is based on an electric circuit with two parallel branches: one for the electrical behaviour and one for the mechanical behaviour. Its implementation in a circuit simulator is very fast and can give good results if the piezoelectric plate is used at a frequency close to its resonant frequency. If the behaviour of the piezoelectric plate must be analysed far from the resonant frequency, it is possible to add parallel branches to take into account higher resonances. However, the main drawback is that the electrical components of this model do not represent propagation of acoustic waves. Mason's model was proposed in the 1950s and is based on a representation of the piezoelectric plate by a three-port electrical circuit, taking into account at the same time the electrical behaviour and the propagation of acoustic waves in one dimension. It requires selection of the right vibration mode in order to use the right electrical circuit. The main drawback of Mason's model is that electrical and mechanical losses are not taken into account. For this purpose, the transmission line model based on Mason's model takes into account all losses in the piezoelectric plate. The model for the thickness vibration mode of a piezoelectric plate is represented in **Figure 17(a)**. Furthermore, it is possible to model all materials by a two-port network as shown in **Figure 17(b)**. The transmission line matrix model can also be used for SAW transducers [26].

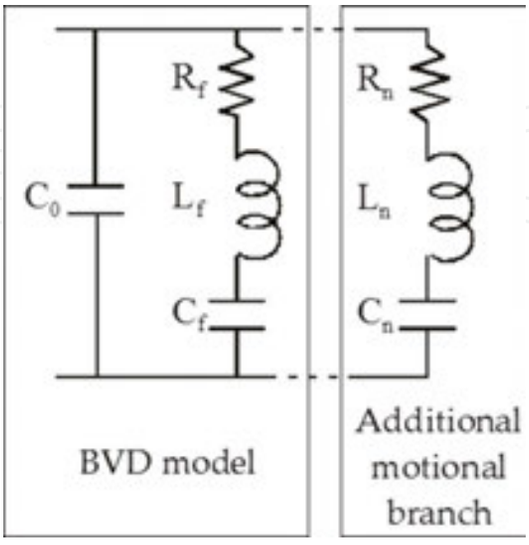


Figure 16. BVD model with additional motional branch.

http://dx.doi.org/10.5772/63125

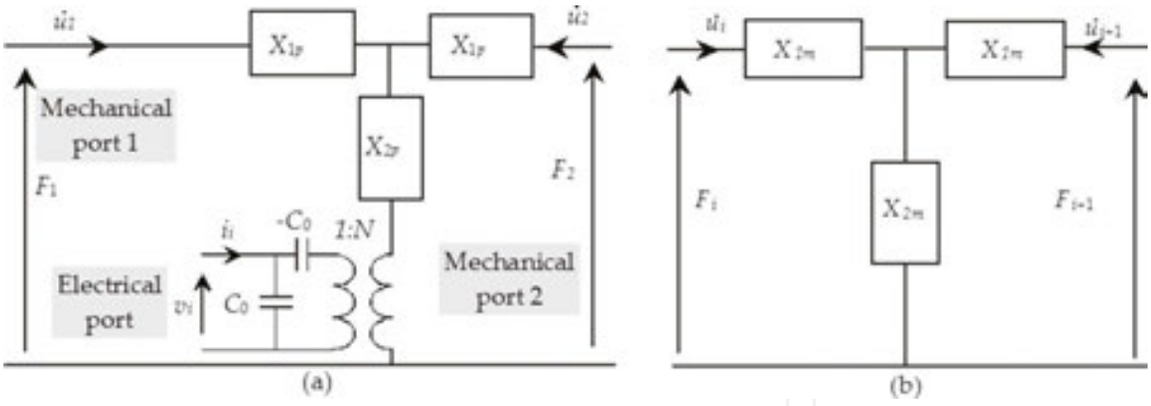


Figure 17. (a) Model of piezoelectric plate in thickness mode. (b) Model of non-piezoelectric layers.

In **Figure 17(a)**, C_0 is the static capacitor obtained by the following plane capacitor formula:

$$C_0 = \frac{\varepsilon_{33}(1 - j\tan\delta_e)S_p}{t_p} \tag{1}$$

The impedances X_{1p} and X_{2p} are given by the following equations:

$$X_{1p} = jZ_pS_p \tan\left(\frac{\omega t}{2v_p}\right) \text{ and } X_{2p} = \frac{Z_pS_p}{j\sin\left(\frac{\omega t}{v_p}\right)} \tag{2}$$

where Z_p, S_p, v_p and t are the acoustic impedance, surface, longitudinal acoustic wave velocity and thickness, respectively, of the piezoelectric layer. With $Z_p = \rho_p V_p$ or $Z_p = \sqrt{c_{33}(1 + j\tan\delta_m)/\rho_p}$, the acoustic impedance of the piezoelectric material for longitudinal waves and V_p is the longitudinal wave velocity in the AlN. The turn ratio of the transformer N is given by the following relationship, where e_{33} is the piezoelectric constant:

$$N = \frac{e_{33}S_p}{t_p} \tag{3}$$

Non-piezoelectric materials (**Figure 17(b)**) are represented as a transmission line with the elastic impedances X_{1m} and X_{2m} corresponding to the following:

$$X_{1m} = jZ_mS_m \tan\frac{\omega t_m}{2V_m} \text{ and } X_{2m} = \frac{Z_mS_m}{j\sin\frac{\omega t_m}{V_m}} \tag{4}$$

with $Z_m = \rho_m V_m$ being the acoustic impedance of each layer, V_m the longitudinal wave velocity, t_m the thickness and ρ_m the density. Mechanical losses are considered in each material in the expression of V_m, which is proportional to the complex elastic constant of the considered material. The surface S_m involved in the model is equal to the active surface of the piezoelectric plate S_p.

The last interesting feature of electrical models is that they can be implemented in electric and RF simulators, such as ADS from Keysight. It allows for use of all possible simulations available in this class of simulators, such as *S* parameters, which allow electromagnetic wave propagation and electrical impedance matching with input and output ports of the filter to be taken into account, harmonic balance simulation or transient simulation.

2.5. Characterisation methods

There are two main methods for characterising filters. The first method is based on time domain analysis, whereas the second is based on frequency measurement. Recently, a pseudo-time method was introduced to perform tests. The first method is based on time domain reflectometry/transmission (TDR/T). It involves sending through the filter a short pulse whose duration is selected to reach the frequency of the filter passband. The reflected and/or transmitted signals are then measured and analysed to obtain the filter behaviour and its time response. Fast Fourier Transform (FFT) could also be used to obtain the frequency response. However, this method requires generating a short pulse and a fast sampling rate. This type of apparatus can be expensive and the obtained measurement does not give better accuracy. This method is seldom used and will not be presented here.

2.5.1. Low power characterisation of S parameters

Measurement of *S* parameters is performed by using a vector network analyser (VNA). This is one of the best ways to characterise a filter. This measurement method is a component of frequency domain analysis as the VNA sweeps a pure sine signal from a start frequency to a stop frequency, which are defined by the user. It requires an initial calibration step and a second step to de-embed access lines and/or pads. After all these operations, the component *S* parameters can be analysed and compared with the desired or ideal characteristics. The obtained *S* parameters are composed of numerous frequency measurement points, generally several hundreds, and for each *S* parameter, the module and the phase or the real part and the imaginary part. This method is used both in research laboratories and in industry. In research laboratories, it allows piezoelectric parameters as well as other parameters to be extracted, although it must be linked to a model of the piezoelectric structure or filter. In the industry, the VNA is used, but it is a time-consuming apparatus because several steps are required before getting the *S* parameters. Furthermore, analysis of *S* parameters must be done to ensure that the devices respond to the desired characteristics. Thus, the cost of the device increases with the analysis time and the type of setup.

http://dx.doi.org/10.5772/63125

2.5.2. High power characterisation

piezoelectric materials used to realise filters can be submitted to high RF power compared with their micrometric dimensions in compact structures [18]. For example, the maximum power emitted by most mobile phones can reach 2 W or 33 dBm. Submitted to this high power, the first resonator of a filter will exhibit a nonlinear behaviour. It is important first to characterise the filter with this high power and next to extract the nonlinear changes of the material constants, such as the piezoelectric constant, the permittivity or the elastic constant.

Two types of measurement can be done. The first is the third-order intercept point (IP_3) measurement, and the second is the 1 dB compression point. For the IP_3 measurement, two sine tones of closed frequencies are combined and applied at the input of the filter. When nonlinear behaviour becomes important, the two frequencies will create an intermodulation and thus an unwanted spurious frequency only due to high power. A measurement configuration type is shown in **Figure 18**.

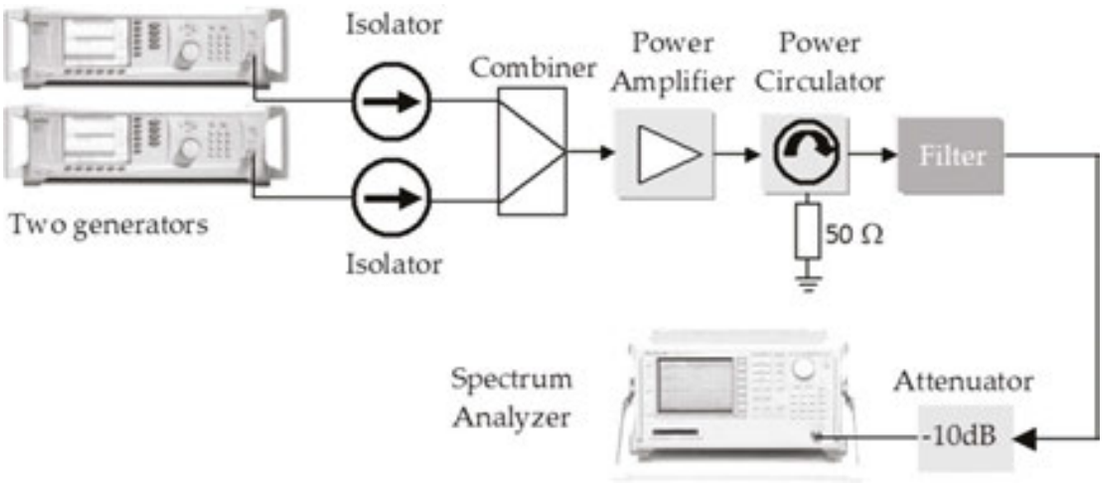


Figure 18. Experimental setup for intercept point measurement.

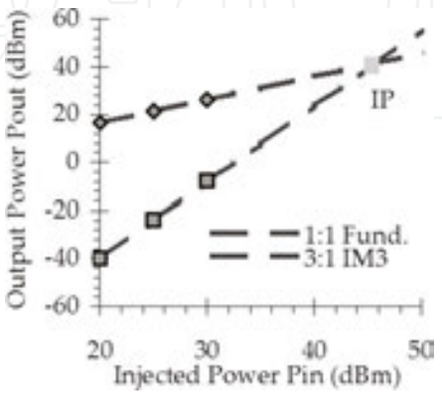


Figure 19. IP_3 measurement.

Signals coming from generators are combined, amplified and applied at the input of the filter. At the output of the filter, a spectrum analyser is used to measure the amplitude of each frequency generated by the generators and the frequencies coming from the intermodulation. Then the output power is represented as the function of the input power for the fundamental frequency and for the third harmonic. The point at the intersection of both lines gives the IP_3 point. An example is given in **Figure 19**.

A VNA must be used to measure the compression point at 1 dB. The principle is to measure the transmission coefficient (S_{21}) as the function of the input power at a fixed frequency, in general the central frequency of the filter passband. A sample measurement setup is given in **Figure 20**. Port 1 is dedicated for excitation, whereas port 2 measures the output signal of the filter. With a directional coupler, the input power of the filter can be obtained and is measured by the reference port of the VNA. A special configuration of the VNA allows for the results shown in **Figure 21** to be obtained directly, where P_1 is the 1 dB compression point. P_1 allows the input power to be determined when the output level decreases by 1 dB as compared with small input power. In most cases, this input power is considered to be the maximum allowable power before reaching the nonlinear behaviour.

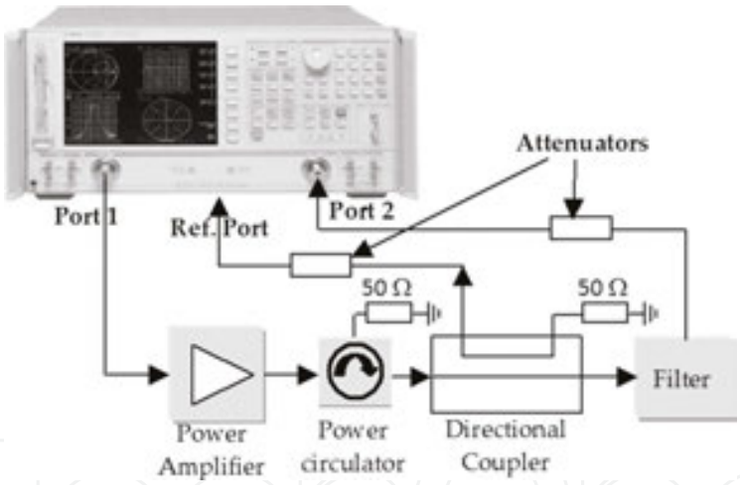


Figure 20. Experimental setup for 1 dB compression point measurement.

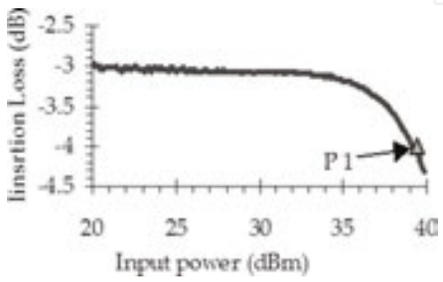


Figure 21. Insertion loss measurement at a fixed frequency and 1 dB compression measurement.

High power measurements can be used to acquire the behaviour of the filter, but also associated with a model, it is possible to extract the variations of the main parameters in the function of power. This was performed for AlN by Sahyoun et al. [27].

2.5.3. Test of filter

The characterisation of filters using a VNA is a good way to obtain much information about the behaviour of structures. Nevertheless, when devices must be tested after fabrication, this kind of measurement is time-consuming and requires the calibration of the VNA after the exploitation of the measured data. An interesting alternative is to perform a test in order to verify if the filter can be used or not with only one measurement and with a more simple measurement setup. Another requirement can be to determine the behaviour in conditions close to the real conditions of operation. For this purpose, a digitally modulated signal can be used. The carrier frequency can be tuned in the passband of the filter, and a QPSK modulated signal is the best trade-off to perform the test. It is possible by analysing the output signal to see if the filter responds to a minimum requirement in terms of insertion losses and passband. This technique presented by Sahyoun et al. [28] offers the possibility to discriminate filters.

3. Piezoelectric MEMS in RF circuits

3.1. Switches and matrixes

This section describes MEMS switches. These devices use mechanical movement to achieve an open or short circuit in the RF transmission line. RF MEMS switches are the specific micromechanical switches designed to operate at RF-to-millimeter wave frequencies (0.1–100 GHz). The forces required for the mechanical movement can be obtained using electrostatic, magnetostatic, thermal or piezoelectric designs. Even if most MEMS RF switches are electrostatic-type switches [29], new switch topologies, based on piezoelectric topology, are now available.

The first piezoelectric material used to design switches has been AlN. Fully integrated RF MEMS switches [30] with piezoelectric actuation have been designed, fabricated and characterised using silicon bulk technology. First a resistive switch having a pure gold metal contact. The measured isolation and insertion loss of the resistive switch are −62 and −0.8 dB at a frequency of 5 GHz, respectively, for an actuation voltage of 3.5 V. A second capacitive switch exhibits an isolation of −18 dB and an insertion loss of −0.7 dB at a frequency of 5 GHz. The isolation curve of the capacitive switch is very flat over a very wide frequency range, from 0.5 to 30 GHz.

Another fully integrated RF MEMS switch with piezoelectric (PZT) actuation has been proposed and characterised by Lee et al. [31]. This switch is composed of a piezoelectric cantilever actuator with a floated contact electrode and isolated CPW transmission line suspended above the silicon substrate. The measured insertion loss and isolation are −0.22 and −42 dB at a frequency of 2 GHz, respectively. The main innovation of this switch is its very low actuation voltage of 2.5 V, instead of around 6–7 V, for more efficient electrostatic switches.

Another paper described a higher frequency switch that uses piezoelectric actuators [32]. This switch is based on a thin film spun of PZT deposited onto a high-resistivity silicon substrate with coplanar waveguide transmission lines (**Figure 22**). Actuation voltages less than 10 V with switch operation demonstrated as low as 2 V. The series switch exhibits better than 20 dB isolation from DC up to 65 GHz and an insertion loss less than 1 dB up to 40 GHz. A new design from the same research team improves PZT switch performances at 10 V with better than 30 dB isolation and an insertion loss less than 0.5 dB from DC to 50 GHz [33].

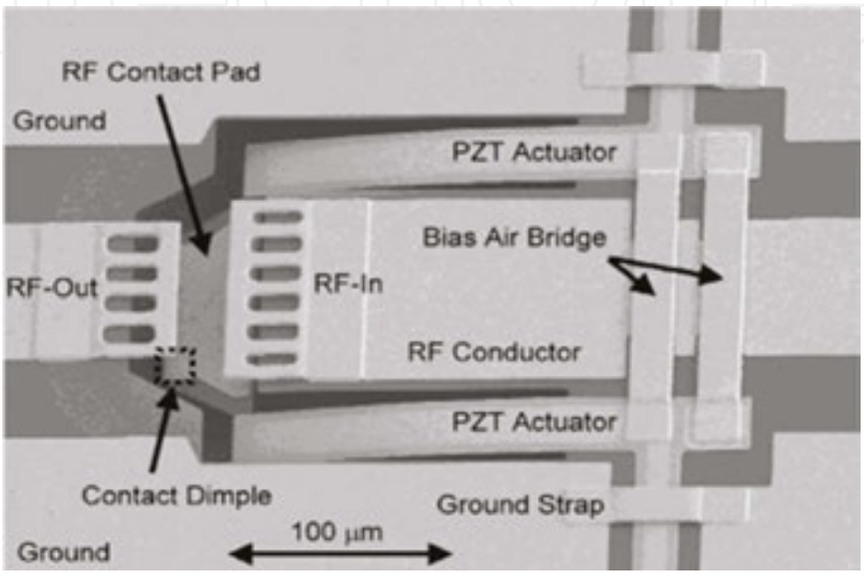


Figure 22. PZT series switch.

Another feature of great interest in this switch technology is the opportunity to report on wafer-level transfer technologies to integrate PZT-based RF MEMS switches into CMOS, as described by Guerre et al. [34]. Such heterogeneous integration can overcome the incompatibility of PZT materials with back-end-of-the-line (BEOL) CMOS technology. Switch characterisation draws out an insertion loss of less than 0.5 dB and an isolation better than 30 dB for the 0.4–6 GHz frequency range with 15 V actuation voltage.

In addition, these low loss and low actuation voltage piezoelectric switches can be correlated to realise a more complex commutation matrix: SP2T (Single Pole Two Throw) and SP4T (Single Pole Four Throw). For example, in the work of Chung et al. [35], as shown in **Figure 23**, from DC to 50 GHz, the overall performance of the switches shows better than 20 dB isolation up to 50 GHz when the MEMS switches are in the off or zero-volt state. When the switches are actuated with 7 V, the SP2T shows less than 1.8 dB of insertion loss while the SP4T shows less than 2 dB of insertion loss, on average, up to 40 GHz.

Some original application associated piezoelectric filters and switches together. Hummel et al. [36] demonstrated an innovative technology platform based on the monolithic integration of AlN resonators and PCM switches that is capable of delivering highly reconfigurable RF components, enabling new radio architectures with enhanced spectrum coverage.

http://dx.doi.org/10.5772/63125

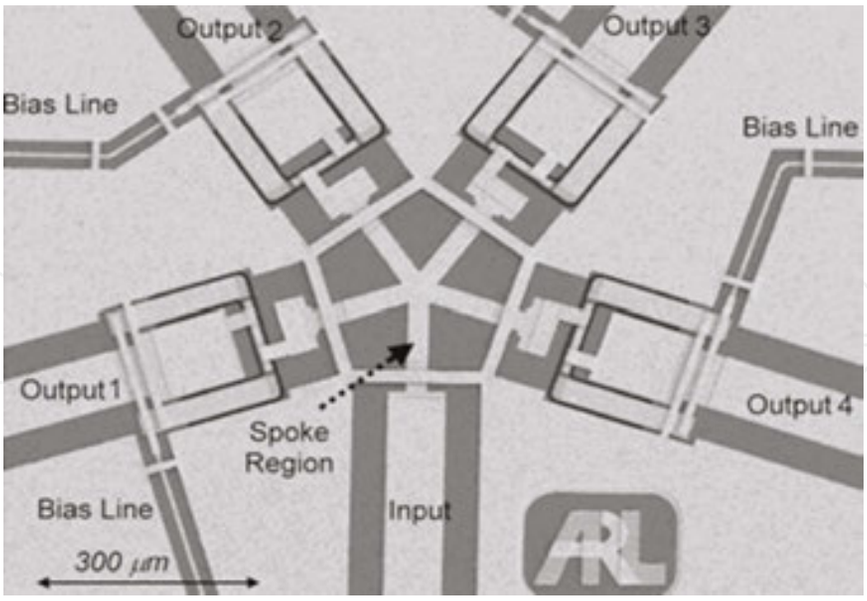


Figure 23. Layout of the SP4T junction with PZT RF MEMS switches.

3.2. Phase shifters

Recent advances in piezoelectric actuated RF MEMS switches allow for the design of more complex functions and at present highly required phase shifters. A 2-bit MEMS phase shifter incorporating PZT switches has been presented by Polcawich et al. [33]. A picture of the layout of the 2-bit phase shifter based on PZT shunt switches is detailed in **Figure 24(a)**. The phase parameters have been measured against the frequency for the four configurations and are

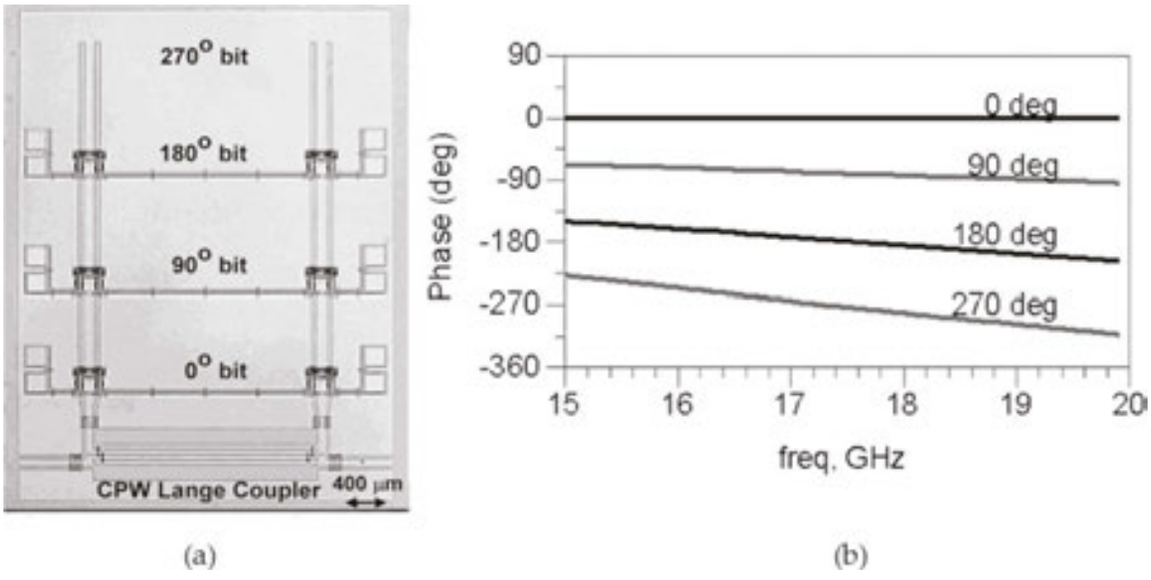


Figure 24. (a) A 17 GHz 2-bit reflection-type phase shifter incorporating PZT shunt switches. (b) Measured normalised phase response.

presented in **Figure 24(b)**. In addition, this phase shifter has an average insertion loss of 2.96 dB using PZT shunt switches operating at 15 V.

A second topology (**Figure 25**) of a 2-bit phase shifter based on two SP4T switch with piezoelectric MEMS switches with a compact 3D passive design on a liquid crystal polymer (LCP) organic substrate was described by Chung et al. [37]. A picture of the complete layout is shown in **Figure 25(a)**. The block diagram presented in **Figure 25(b)** describes the principle based on two SP4T switch matrixes. The transmission phase measured results are detailed in **Figure 25(c)**. The multilayer LCP process allows a low-cost and lightweight circuit that can easily be integrated with other RF front-end components, such as an antenna, at the packaging level.

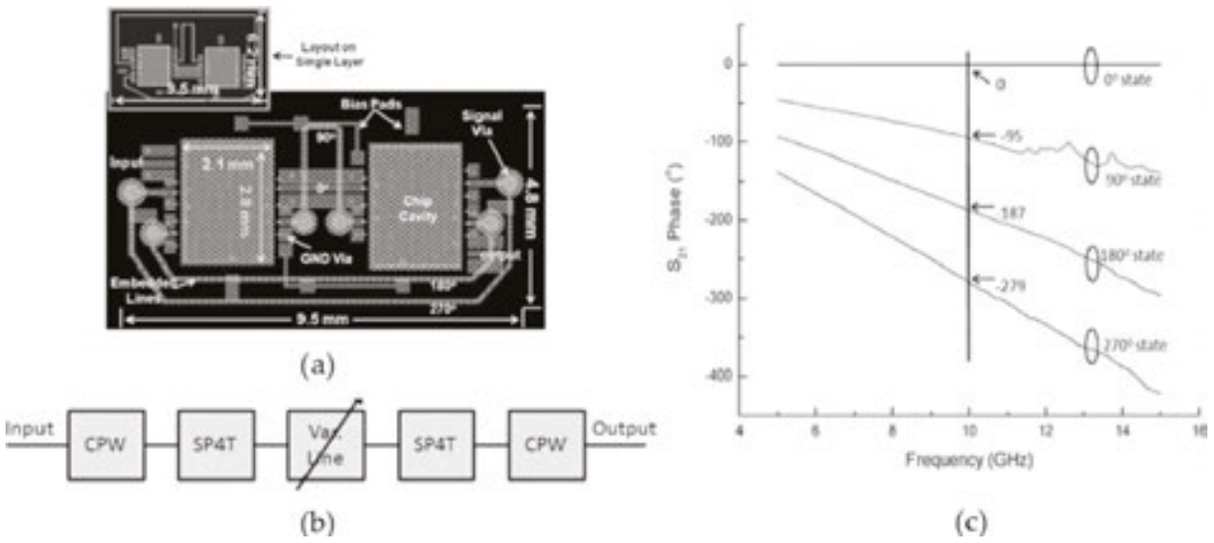


Figure 25. Proposed 3D phase shifter. (a) Layout with size comparison with a phase shifter with its footprint on a single layer. (b) Corresponding block diagram and measured normalised phase response of the 3D phase shifter. (c) Measured normalised phase response of the 3D phase shifter.

3.3. RF varactors

RF MEMS devices are competitive for handling high-frequency microwave signals. In comparison with semiconductor devices, the performance of RF MEMS devices is highly linear, minimising signal distortion.

A 3 V operation RF MEMS variable capacitor using hybrid actuation of piezoelectric and electrostatic forces was presented by Ikehashi et al. [38] and Ikehashi et al. [39]. An image of this varactor is presented in **Figure 26(a)**. The measured capacitance ratio is $C_{max}/C_{min} = 14$. The hybrid actuation and the optimised bending enabled 2.6 V pull-in voltage, with the pull-out voltage as high as 2.0 V, as shown in **Figure 26(b)**. The piezoelectric actuator, which uses thin film PZT, enabled low voltage actuation, while the electrostatic actuator realised a large capacitance ratio.

http://dx.doi.org/10.5772/63125

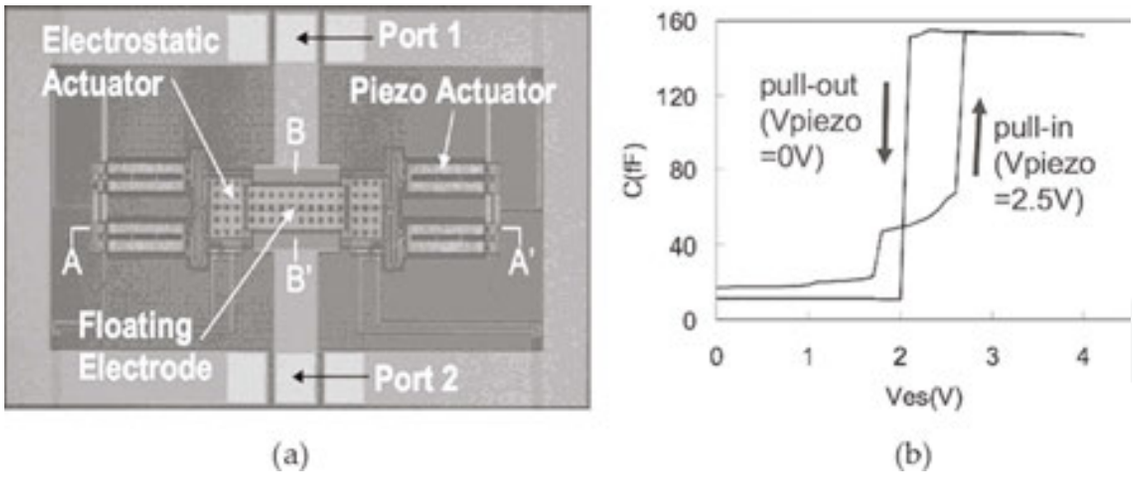


Figure 26. (a) Top view of the variable capacitor. (b) *V* hysteresis curve with V_{piezo} values of 2.5 and 0 V during pull-in and pull-out, respectively.

4. Conclusion and prospects

The need for piezoelectric materials for RF applications will continue to grow. Some important features must be taken into account in the future: Lead-free materials are necessary, as lead must be removed from almost all devices. Future devices will be tunable in order to reduce the number of components and to give the possibility of using several standards, particularly in radio transmission systems. As the number of devices to fabricate is important, future materials must be compatible with fabrication processes of micro technologies. The control of the thickness of piezoelectric layers is a great challenge because the cost of the control with good accuracy of this parameter remains high. Finally, testing piezoelectric devices for high-volume manufacturing remains to be explored.

Owing to new piezoelectric materials, innovative RF devices have been designed from a simple resonator or switch to a more complex architecture, such as a phase shifter on a tunable filter. MEMS piezoelectric devices offer promising performances for RF applications. For example, switches allow actuation voltage levels two times smaller than in electrostatic switches and varactors a large capacitance ratio (C_{max}/C_{min} = 14).

Author details

Philippe Benech* and Jean-Marc Duchamp

*Address all correspondence to: philippe.benech@minatec.inpg.fr

IMEP-LAHC Laboratory, Grenoble Alpes University, Grenoble, France

References

[1] Oita T. RF MEMS: Focusing on the next step. Ultrasonics Symposium, pp. 1173–1178, 20–23 September 2009. DOI: 10.1109/ULTSYM.2009.5442083

[2] Tehon S, Wanuga S. Microwave acoustics, in Proceedings of the IEEE, vol. 52, no. 10, pp. 1113–1127, October 1964. DOI: 10.1109/PROC.1964.3298

[3] Yao S, Young E. Properties and applications of composite bulk acoustic resonators. Ultrasonics Symposium, pp. 593–596, 1976. DOI: 10.1109/ULTSYM.1976.196749

[4] Ruby R, Bradley P, Larson I, Oshmyansky JY, Figueredo D. Ultra-miniature high-*Q* filters and duplexers using FBAR technology. Proceedings of First International Solid-State Circuit Conference, San Francisco, CA, USA, February 2001, pp. 120–121. DOI: 10.1109/ISSCC.2001.912569

[5] Matloub R, Artieda A, Sandu C, Milyutin E, Muralt P. Electromechanical properties of $Al_{0.9}Sc_{0.1}N$ thin films evaluated at 2.5 GHz film bulk acoustic resonators. Applied Physics Letters. 2011, 99:092903. DOI: 10.1063/1.3629773

[6] Yokoyama T, Iwazaki Y, Onda Y, Nishihara T, Sasajima Y, Ueda M. Highly piezoelectric co-doped AlN thin films for wideband FBAR applications. IEEE Transactions on Ultrasonics, Ferroelectrics and Frequency Control. 2015, 62(6):1007–15. DOI: 10.1109/TUFFC.2014.006846

[7] Zhu X, Phillips J, Mortazawi A. A DC voltage dependant switchable thin film bulk wave acoustic resonator using ferroelectric thin film. Proceedings of International Microwave Symposium '07, Honolulu, HI, USA, June 2007, pp. 671–674. DOI: 10.1109/MWSYM.2007.380009

[8] Ansari A, Gokhale V-J, Thakar V-A, Roberts J, Rais-Zadeh M. Gallium nitride-on-silicon micromechanical overtone resonators and filters. 2011 IEEE International Electron Devices Meeting, Washington, DC. DOI: 10.1109/IEDM.2011.6131590

[9] Shrout TR, Zhang SJ. Lead-free piezoelectric ceramics: Alternatives for PZT? Journal of Electroceramics. 2007, 19:111–124. DOI: 10.1007/s10832-007-9047-0

[10] Gong S, Shi L, Piazza G. High electromechanical coupling MEMS resonators at 530 MHz using ion sliced X-cut $LiNbO_3$ thin film. Proceedings of International Microwave Symposium, Montreal, Canada, June 2012. DOI: 10.1109/MWSYM.2012.6259767

[11] Kimura T, Kadota M, Ida Y. High *Q* SAW resonator using upper-electrodes on grooved-electrodes in $LiTaO_3$. Proceedings of International Microwave Symposium, Anaheim, CA, USA, May 2010, pp. 1740–1743. DOI: 10.1109/MWSYM.2010.5516895

[12] Hanajima N, Tsutsumi S, Yonezawa T, Hashimoto K, Nanjo R, Yamaguchi M. Ultrasonic properties of lead zirconate titanate thin films in UHF-SHF range. Japan Journal of Applied Physics. 1997, 36:6069–6072. DOI: 10.1143/JJAP.36.6069

[13] Muralt P, Conde J, Artieda A, Martin F, Cantoni M. Piezoelectric materials parameters for piezoelectric thin films in GHz applications. International Journal of Microwave and Wireless Technologies. 2009, 1:19–27. DOI: 10.1143/JJAP.36.6069

[14] Lin CM, Chen YY, Felmetsge VV, Senesky DG, Pisano AP. Two-port filters and resonators on AlN/3C-SiC plates utilizing high-order Lamb wave modes. IEEE International Conference on MEMS, Taipei, Taiwan, January 2013. DOI: 10.1109/MEMSYS.2013.6474361

[15] Hoang T, Vaudaine MH, Danel JS, Robert P, Benech P, Lemaitre-Auger P. Temperature-compensated structure for saw pressure sensor in very high temperature. IEEE International Frequency of Control Symposium, Geneva, CH, May 2007, pp. 40–44. DOI: 10.1109/FREQ.2007.4319026

[16] Kaletta UCh, Santos PV, Wolansky D, Scheit A, Fraschke M, Wipf C, Zaumseil P, Wenger C. Monolithic integrated SAW filter based on AlN for high-frequency applications. Semiconductor Science and Technology. 2013, 28:065013. DOI: 10.1088/0268-1242/28/6/065013

[17] Yamada T, Nakamurat H, Nishimuratt K, Ishizakit T, Ogawat K. A flat-time-delay transversely coupled resonator SAW filter comprising parallel connected filter tracks. IEEE Ultrasonic Symposium, San Juan, Puerto Rico, 2000, pp. 12-124. DOI: 10.1088/0268-1242/28/6/065013

[18] Ivira B, Benech P, Fillit R, Ndagijimana F, Ancey P, Parat G. Modeling for temperature compensation and temperature characterizations of BAW resonators at GHz frequencies. IEEE Transactions on Ultrasonics, Ferroelectrics, and Frequency Control. 2008, 55(2):421–430. DOI: 10.1109/TUFFC.2008.660

[19] Aigner R. MEMS in RF filter applications: Thin-film bulk acoustic wave technology. Sensors Update, 2003, 12, 175–210. DOI: 10.1109/SENSOR.2005.1496345

[20] Reddy PR, Mohan BC. Design and analysis of film bulk acoustic resonator (FBAR) filter for RF applications. International Journal of Radio Frequency Identification and Wireless Sensor Networks. 2012, vol. 4. DOI: 10.5772/50930

[21] ten Dolle HKJ, Lobeek JW, Tuinhout A, Foekema J. Balanced lattice-ladder bandpass filter in bulk acoustic wave technology. International Microwave Symposium, June 2004, Fort Worth, TX, USA, pp. 391–394. DOI: 10.1109/MWSYM.2004.1335904

[22] Lakin KM. Coupled resonator filters. IEEE Ultrasonic Symposium, October 2002, Munich, Germany, pp. 901–908. DOI: 10.1109/ULTSYM.2002.1193543

[23] Fattinger GG, Kaitila J, Aigner R, Nessler W. Single-to-balanced filters for mobile phones using coupled resonator BAW technology. IEEE Ultrasonic Symposium, Montréal, Canada, August 2004, pp. 416–419. DOI: 10.1109/ULTSYM.2004.1417751

[24] Krimholtz R, Leedom DA, Matthaei GL. New equivalent circuit for elementary piezoelectric transducers. Electronics Letters. 1970, 6:398–399. DOI: 10.1049/el:19700280

[25] Sherrit S, Leary SP, Dolgin BP, Bar-Cohen Y. Comparison of the Mason and KLM equivalent circuits for piezoelectric resonators in the thickness mode. Proceedings of IEEE Ultrasonic Symposium, pp. 921–926, 1999. DOI: 10.1109/ULTSYM.1999.849139

[26] Hoang T, Rey P, Vaudaine MH, Robert P, Benech P. The hybrid model for SAW filter. Proceedings of ICECS 2008, pp. 336–339, 31st August–3rd September 2008, Malta. DOI: 10.1109/ICECS.2008.4674859

[27] Sahyoun W, Duchamp JM, Benech P. Acoustic, piezoelectric, and dielectric nonlinearities of AlN in coupled resonator filters for high RF power levels. IEEE Transactions on Ultrasonics, Ferroelectrics, and Frequency Control. 2011, 58:2162–2170. DOI: 10.1109/TUFFC.2011.2065

[28] Sahyoun W, Duchamp JM, Benech P. Validation of EVM method for filter test using Butterworth and Chebyshev filters. IEEE Transaction on MTT, Vol. 64 n°3 pp. 952–960. DOI: 10.1109/TMTT.2016.2518170

[29] Rebeiz GM, Muldavin JB. RF MEMS switches and switch circuits. Microwave Magazine. 2001, 2(4):59–71. DOI: 10.1109/6668.969936

[30] Lee HC, Park JY, Lee KH, Nam HJ, Bu JU. Silicon bulk micromachined RF MEMS switches with 3.5 volts operation by using piezoelectric actuator. IEEE MTT-S International, vol. 2, pp. 585–588, 6–11 June 2004, DOI: 10.1109/MWSYM.2004.1336049

[31] Lee HC, Park JY, Bu JU. Piezoelectrically actuated RF MEMS DC contact switches with low voltage operation. Microwave and Wireless Components Letters. 2005, 15(4), 202–204. DOI: 10.1109/LMWC.2005.845689

[32] Polcawich RG, Pulskamp JS, Judy D, Ranade P, Trolier-McKinstry S, Dubey M. Surface micromachined microelectromechanical ohmic series switch using thin-film piezoelectric actuators. Microwave Theory and Techniques. 2007, 55(12):2642–2654. DOI: 10.1109/TMTT.2007.910072

[33] Polcawich RG, Judy D, Pulskamp JS, Trolier-McKinstry S, Dubey M. Advances in piezoelectrically actuated RF MEMS switches and phase shifters. IEEE/MTT-S International, pp. 2083–2086, 3–8 June 2007. DOI: 10.1109/MWSYM.2007.380297

[34] Guerre R, Drechsler U, Bhattacharyya D, Rantakari P, Stutz R, Wright RV, Milosavljevic ZD, Vaha-Heikkila T, Kirby PB, Despont M. Wafer-level transfer technologies for PZT based RF MEMS switches. Journal of Microelectromechanical Systems. 2010, 19(3):548–560. DOI: 10.1109/JMEMS.2010.2047005

[35] Chung DJ, Polcawich RG, Judy D, Pulskamp J, Papapolymerou J. A SP2T and a SP4T switch using low loss piezoelectric MEMS. IEEE MTT-S International, pp. 21–24, 15–20 June 2008. DOI: 10.1109/MWSYM.2008.4633093

[36] Hummel G, Yu Hui, Rinaldi M. Reconfigurable piezoelectric MEMS resonator using phase change material programmable vias. Journal of Microelectromechanical Systems. 2015, 24(6):2145–2151. DOI: 10.1109/JMEMS.2015.2478710

[37] Chung DJ, Polcawich RG, Pulskamp JS, Papapolymerou J. Reduced-size low-voltage RF MEMS X-band phase shifter integrated on multilayer organic package. Components, Packaging and Manufacturing Technology. 2012, 2(10):1617–1622. DOI: 10.1109/TCPMT.2012.2184112

[38] Ikehashi T, Ogawa E, Yamazaki H, Ohguro T. A 3V operation RF MEMS variable capacitor using piezoelectric and electrostatic actuation with lithographical bending control. Solid-State Sensors, Actuators and Microsystems Conference, 2007. TRANSDUCERS 2007, pp. 149–152, 10–14 June 2007. DOI: 10.1109/SENSOR.2007.4300093

[39] Ikehashi T, Ohguro T, Ogawa E, Yamazaki H, Kojima K, Matsuo M, Ishimaru K, Ishiuchi H. A robust RF MEMS variable capacitor with piezoelectric and electrostatic actuation. IEEE MTT-S, 39–42, pp. 11–16 June 2006. DOI: 10.1109/MWSYM.2006.249903

IntechOpen

IntechOpen

IntechOpen